The ISME Journal (2018) 12, 112–123
www.nature.com/ismej

OPEN

ORIGINAL ARTICLE

DNA-SIP based genome-centric metagenomics identifies key long-chain fatty acid-degrading populations in anaerobic digesters with different feeding frequencies

Ryan M Ziels[1,2], Diana Z Sousa[3], H David Stensel[2] and David AC Beck[4,5]
[1]*Department of Civil Engineering, University of British Columbia, Vancouver, British Columbia, Canada;* [2]*Department of Civil and Environmental Engineering, University of Washington, Seattle, WA, USA;* [3]*Laboratory of Microbiology, Wageningen University, Wageningen, The Netherlands;* [4]*eScience Institute, University of Washington, Seattle, WA, USA and* [5]*Department of Chemical Engineering, University of Washington, Seattle, WA, USA*

Fats, oils and greases (FOG) are energy-dense wastes that can be added to anaerobic digesters to substantially increase biomethane recovery via their conversion through long-chain fatty acids (LCFAs). However, a better understanding of the ecophysiology of syntrophic LCFA-degrading microbial communities in anaerobic digesters is needed to develop operating strategies that mitigate inhibitory LCFA accumulation from FOG. In this research, DNA stable isotope probing (SIP) was coupled with metagenomic sequencing for a genome-centric comparison of oleate ($C_{18:1}$)-degrading populations in two anaerobic codigesters operated with either a pulse feeding or continuous-feeding strategy. The pulse-fed codigester microcosms converted oleate into methane at over 20% higher rates than the continuous-fed codigester microcosms. Differential coverage binning was demonstrated for the first time to recover population genome bins (GBs) from DNA-SIP metagenomes. About 70% of the ^{13}C-enriched GBs were taxonomically assigned to the *Syntrophomonas* genus, thus substantiating the importance of *Syntrophomonas* species to LCFA degradation in anaerobic digesters. Phylogenetic comparisons of ^{13}C-enriched GBs showed that phylogenetically distinct *Syntrophomonas* GBs were unique to each codigester. Overall, these results suggest that syntrophic populations in anaerobic digesters can have different adaptive capacities, and that selection for divergent populations may be achieved by adjusting reactor operating conditions to maximize biomethane recovery.
The ISME Journal (2018) **12,** 112–123; doi:10.1038/ismej.2017.143; published online 12 September 2017

Introduction

Anaerobic digestion is an attractive biotechnology for recovering renewable energy as biomethane (CH_4) during organic waste treatment. Worldwide interest in anaerobic digestion has led to the implementation of ~ 9000 full-scale facilities in Europe and over 3000 facilities in the US by 2012 (Guo *et al.*, 2015). The conversion of organic matter into biomethane relies upon an intricate balance of multiple microbial trophic groups, including hydrolyzing and fermenting bacteria, syntrophic acetogenic bacteria and methanogenic archaea (Briones and Raskin, 2003). Despite the relatively widespread adoption of anaerobic digestion, the variety of its contributing genetic and metabolic systems still remain relatively underexplored (Vanwonterghem *et al.*, 2016), owing to the vast phylogenetic and metabolic diversity (Sundberg *et al.*, 2013) and general non-culturability of a majority of the microorganisms present in digesters (Vanwonterghem *et al.*, 2014). An improved understanding of the key ecological niches within anaerobic digesters and the metabolic and physiological attributes of microbial populations occupying those niches could help to facilitate new process designs and operational strategies that maximize biomethane recovery from organic waste.

Adding fats, oils and greases (FOG) as a co-substrate during the anaerobic digestion of livestock manure or wastewater treatment solids has gained popularity to increase biomethane recovery due to the high biological methane potential of FOG (Alves *et al.*, 2009; Luostarinen *et al.*, 2009; Wang *et al.*, 2013). During anaerobic degradation, FOG is rapidly

Correspondence: RM Ziels, Department of Civil Engineering, University of British Columbia, 2017 Applied Science Lane, Vancouver, British Columbia, Canada V6T 1Z4.
E-mail: ziels@mail.ubc.ca
Received 24 April 2017; revised 22 June 2017; accepted 22 July 2017; published online 12 September 2017

hydrolyzed into glycerol and long-chain fatty acids (LCFA) (Hanaki *et al.*, 1981). Because the degradation of LCFA in methanogenic environments relies on low hydrogen, formate and acetate levels for favorable thermodynamics, LCFA are converted into methane through an obligatory syntrophic partnership between acetogenic β-oxidizing bacteria and methanogenic archaea (Schink, 1997; Sousa *et al.*, 2009). So far, only seven isolated bacterial species are capable of β-oxidizing LCFA (>12 carbons in length) in syntrophy with methanogens, and all belong to the families of *Syntrophomonadaceae* and *Syntrophaceae* (Sousa *et al.*, 2009; Zhang *et al.*, 2012). However, the generally slow growth rates of syntrophic bacteria coupled with the toxicity of LCFA has limited the number of cultured representatives obtained (Hatamoto *et al.*, 2007).

Biomethane recovery from FOG can be limited by the reduction of microbial activity attributed to the toxicity of LCFAs at high concentrations (Hanaki *et al.*, 1981; Angelidaki and Ahring, 1992; Rinzema *et al.*, 1994; Davidsson *et al.*, 2008; Luostarinen *et al.*, 2009; Wan *et al.*, 2011; Wang *et al.*, 2013). Our recent work indicated that the maximum FOG loading rate to an anaerobic codigester was dependent on the LCFA-degrading population abundance and specific LCFA bioconversion kinetics (Ziels *et al.*, 2016, 2017). The codigester LCFA feeding frequency was found to impact the composition and diversity of β-oxidizing *Syntrophomonas* species, with LCFA pulse feeding leading to higher bioconversion kinetics in comparison to semi-continuous LCFA feeding (Ziels *et al.*, 2017). However, those detected differences in the syntrophic community structure between codigesters were based on time-series 16S rRNA gene amplicon sequencing, and thus the impact of feeding frequency on the active fraction of the community remained unknown. A comparison of the active LCFA-degrading populations selected with different feeding frequencies would improve our understanding of relationships between operating parameters and physiological diversity within digester syntrophic populations.

Stable isotope probing (SIP) is a cultivation-independent method that can be used to elucidate links between microbial activity (function) and identity within environmental samples (Radajewski *et al.*, 2000; Dumont and Murrell, 2005). DNA-SIP relies on the incorporation of heavy isotopes (for example, ^{13}C) into microbial DNA during growth on labeled substrates, and thus acts as a 'filter' to enrich the DNA of active populations (Chen and Murrell, 2010). DNA-SIP has been combined with shotgun metagenomic sequencing approaches to discover novel enzymes and operons within microbial communities (Saidi-Mehrabad *et al.*, 2013; Chemerys *et al.*, 2014; Verastegui *et al.*, 2014), and to identify new functional traits of microbial taxa (Eyice *et al.*, 2015). Recently-developed differential coverage binning techniques for recovering population genomes from shotgun metagenomes (Albertsen *et al.*, 2013; Kang *et al.*, 2015; Karst *et al.*, 2016) could be amenable to DNA-SIP due to the expected DNA sequence composition divergence between heavy density fractions of ^{12}C- and ^{13}C-incubated samples (Coyotzi *et al.*, 2016). However, there have been no reported studies coupling differential coverage binning with DNA-SIP to recover population genome bins from metagenome sequence data thus far.

The objective of this study was to apply DNA-SIP combined with shotgun metagenomic sequencing for a genome-centric comparison of the active oleate ($C_{18:1}$ LCFA) degrading populations in two parallel anaerobic codigesters operated with different oleate feeding frequencies. Differential coverage binning was employed to retrieve population genome bins from the DNA-SIP ^{13}C and ^{12}C-metagenomes. 16S rRNA gene amplicon sequencing was also conducted on ^{13}C and ^{12}C heavy DNA fractions to verify key populations involved in converting oleate into biomethane within the anaerobic codigesters.

Materials and methods

Anaerobic bioreactor operation

To examine the selective impacts of feeding frequency on the microbial community, two parallel anaerobic codigesters treating manure and oleate were operated at 35 °C for over 200 days, as described previously (Ziels *et al.*, 2017). The digesters had a 4-liter working volume and a 20-day hydraulic and solids retention time (SRT), and were fed with blended manure feedstock collected from a nearby dairy farm. Manure was fed daily at a VS loading rate of 1.3 ± 0.2 g VS/l-d, and an aqueous solution of sodium oleate (>97%, Tokyo Chemical Industry Co.) was added to the influent feed at 10% of the daily feed volume. The daily average oleate organic loading rate (OLR) to both codigesters was identical, but their oleate feeding frequency differed. One codigester received the oleate feed semi-continuously every 6-h, and is termed the continuous-fed (CF) codigester. The other codigester received the oleate feed in a pulse every 2 days, and is termed the pulse-fed (PF) codigester. At day 205 of operation, the oleate OLR to both codigesters was reduced from 3.2 to 1.8 g COD/l-d to promote stable digestion, as acetate was accumulating in the CF codigester effluent by day 200 (Ziels *et al.*, 2017). The resulting oleate concentration in the feed was 44 mM after day 205. From days 205–230, the pH of both codigesters averaged 7.5, and effluent VFA (acetate) was below 400 mg l^{-1}. The codigesters were not fed between days 228-230 to reduce the level of any background substrates before commencing SIP incubations on day 230. At that time, total effluent VFA and LCFA (liquid+sorbed) levels were below 70 mg l^{-1}.

Stable isotope probing incubations with anaerobic digester sludge

Sludge was sampled directly from the PF and CF codigesters on day 230. Microcosms were

established in 35 ml glass serum bottles pre-purged with N_2:CO_2 (80:20), amended with 10 ml of codigester sludge (0.17 g VS total), sealed and capped with butyl rubber septa, and purged again with N_2:CO_2 (80:20). All microcosms were maintained at 35 °C, and stirred at 150 rpm on an orbital shaker. Microcosms were grouped into duplicate vials that were supplemented with either ^{12}C-sodium oleate or ^{13}C-labeled sodium oleate at an initial concentration of 8 mM. The ^{13}C-labeled sodium oleate was universally labeled at all 18 carbons (>98% atom purity, Cambridge Isotope Laboratories, Tewksbury, MA, USA). Triplicate un-supplemented controls were incubated in parallel to measure background methane production. Gas production was measured based on the headspace pressure increase using a digital manometer (Series 490 A, Dwyer Instruments), and the headspace methane content was measured with a GC-FID (SRI 8610C) equipped with a Supelco Alumina Sulfate Plot column (50 m, 0.53 mm i.d.). Headspace pressure and composition were sampled about every 5 h using sterile syringes. Background methane production was subtracted from oleate-amended assays to measure the overall rate of substrate conversion.

After the first addition of oleate was converted at >95% efficiency into methane over 48 h (Figure 1), ^{12}C- and ^{13}C-labeled sodium oleate were re-supplemented at 8 mM after purging the headspace with N_2:CO_2 (80:20). Following another 48-h for oleate conversion into methane, a third supplement of 8 mM ^{12}C- and ^{13}C-labeled sodium oleate was added to the microcosms after purging the headspace with N_2:CO_2 (80:20). The third incubation lasted 48 h, after which biomass from all bottles was sacrificed for DNA extraction. In total, 240 µmol of either ^{12}C- or ^{13}C-labeled oleate was added to the microcosms over the course of 6 days (144 h).

DNA extraction and density-gradient centrifugation

Anaerobic codigester sludge samples were collected for DNA extraction at the start of the SIP incubation (time zero), as well as from each ^{12}C-oleate and ^{13}C-oleate fed microcosm after 6 days of incubation. DNA was extracted and subjected to density-gradient centrifugation and fractionation, as described in detail in the Supplementary Information.

Quantitative PCR

To further detect differences in DNA buoyant density (BD) values between the ^{12}C- and ^{13}C-incubated microcosms, quantitative PCR (qPCR) was conducted on DNA from gradient fractions with BDs ranging from 1.68 to 1.75 g ml^{-1}. The qPCR targeted 16S rRNA gene fragments of the syntrophic LCFA β-oxidizing bacterial genus of *Syntrophomonas* using primers and probes developed by Ziels *et al.* (2015). More detailed descriptions of the reaction

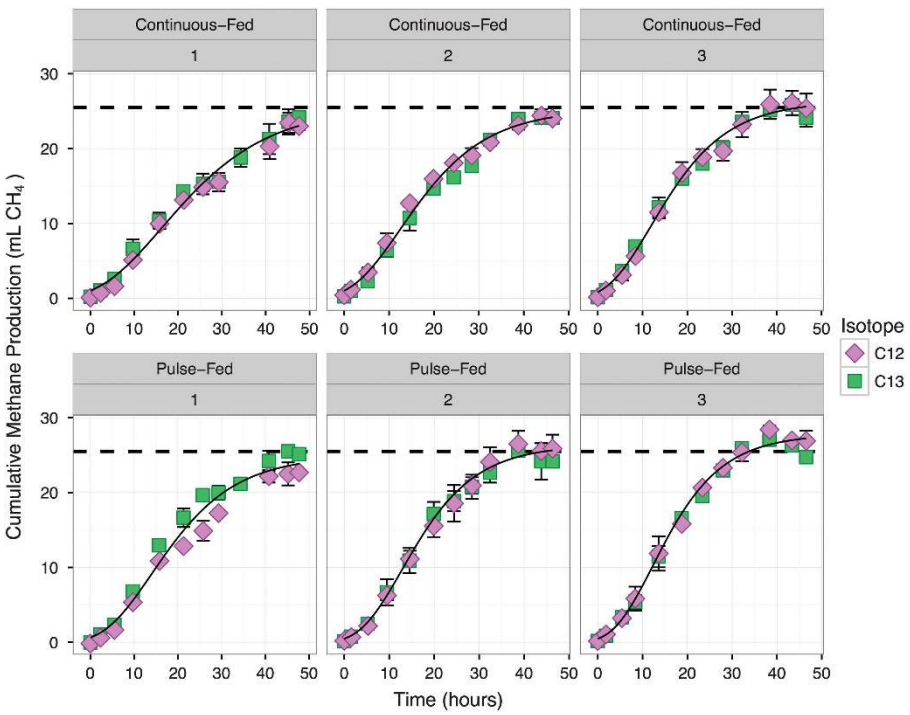

Figure 1 Cumulative methane production (minus blank controls) for the microcosms fed with ^{12}C- and ^{13}C-labeled oleate over three repeated batch feeding periods. The number above each plot indicates the batch oleate feed round. The black dashed line shows the theoretical methane potential of the added oleate (25.5 ml CH_4; based on 2.9 g COD/g oleate, 8 mM concentration and 35 °C temperature). The black solid line represents the predicted methane production based on non-linear model fitting with a modified Gompertz equation (Supplementary Table 1). Error bars represent the standard deviation of the biological replicates.

conditions, primers and probes, and calibration standards are given in the Supplementary Information.

16S rRNA gene amplicon sequencing

DNA from 'heavy' gradient fractions with BDs ranging from 1.70 to 1.73 (4 fractions) were pooled at equal volumes and subjected to 16S rRNA gene amplicon sequencing for each microcosm (Figure 2). Briefly, 16S rRNA gene fragments were amplified with barcoded and indexed universal prokaryotic V4-V5 primers 515 F-Y (5′-GTGYCAGCMGCCGCGGTAA) and 926 R (5′-CCGYCAATTYMTTTRAGTTT) (Parada *et al.*, 2016), and the products were pooled and sequenced on a 2x300 bp Illumina MiSeq run by the United States Department of Energy (DOE) Joint Genome Institute (JGI). Raw sequence data is available through the JGI Portal (http://jgi.doe.gov) under project ID number 1105527.

Amplicon reads were denoised into their exact sequences using the DADA2 pipeline v.1.2.1 (Callahan *et al.*, 2016) before clustering into 99.5% OTUs with UPARSE v.8.1 (Edgar, 2013), as described in detail in the Supporting Information.

Metagenomic sequencing, assembly and annotation

Pooled volumetric fractions of heavy DNA from density-gradient centrifugation (Figure 2), as well as codigester DNA samples from time zero, were used to generate an Illumina sequence library with an average insert size of 250 bp that was sequenced on an Illumina HiSeq-2500 with paired-end 150 bp reads at the DOE JGI. The metagenomic sequencing produced an average of 88 ± 11 M reads for SIP DNA samples and 140 ± 13 M reads for time zero DNA samples. Reads were trimmed and screened to remove adapters as well as filter sequences with a minimum Phred quality of 12, minimum length of 51 and no ambiguous bases using BBDuk v.36.02 (https://sourceforge.net/projects/bbmap/). Trimmed and screened paired-end reads from the codigester time zero metagenomes were individually assembled into contigs using MEGAHIT v.1.0.3 (Li *et al.*, 2015a) with default parameters and the kmer list: 23, 43, 63, 83, 103, 123. The assembled contigs were annotated with the Integrated Microbial Genomes Metagenome (IMG/M) platform (Chen *et al.*, 2016) by the DOE JGI, and KEGG annotation information (KO and EC numbers) were extracted. Raw sequence reads and assemblies are available through the DOE JGI portal under project IDs 1105480, 1105482, 1105484, 1105486, 1105488, 1105490, 1105494, 1105496 and 1105498.

Metagenomic binning

Quality-filtered reads from all metagenomes, including the heavy gradient fractions of the ^{12}C- and ^{13}C-oleate fed microcosms and from codigester time zero

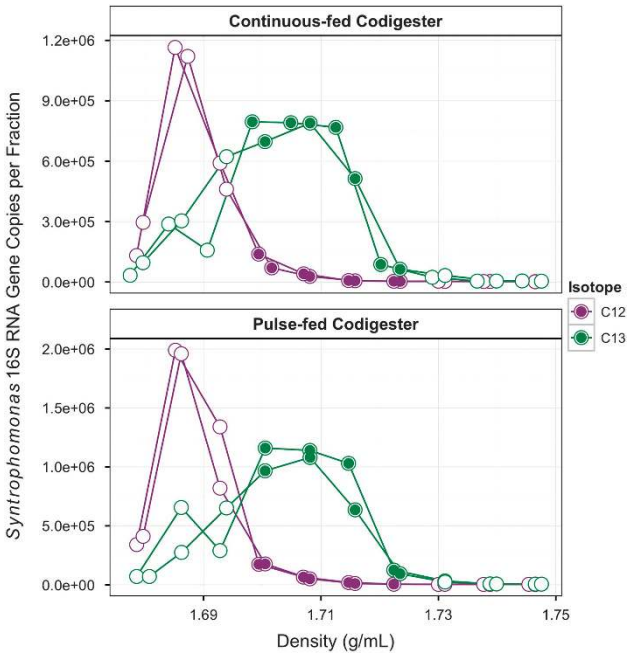

Figure 2 Total copies of *Syntrophomonas* 16S rRNA genes measured by qPCR for each density-gradient fraction recovered from isopycnic separation of DNA from ^{13}C-incubated microcosms and ^{12}C-controls for both anaerobic codigesters. The filled circles indicate gradient fractions that were pooled for subsequent 16S rRNA gene amplicon sequencing and metagenomic sequencing. Both biological replicate microcosms are shown, and each point represents an average of duplicate technical replicates.

samples, were individually mapped to contigs from the time zero assemblies using BBMap v.36.02 (https://sourceforge.net/projects/bbmap/) in paired-end mode with default parameters. SAMtools v.1.4 (Li *et al.*, 2009) was used to sort and index the mapping files and extract contig coverage information across samples. The mapping data and coverage information were used to bin contigs into population genome bins (GBs) separately for each codigester sample set using MetaBat v.0.26.3 (Kang *et al.*, 2015) in 'superspecific' mode. CheckM v.1.0.6 was used to evaluate the level of bin completeness and contamination based on domain-level single-copy marker genes (Parks *et al.*, 2015). Taxonomic classification of GBs was conducted by extracting a set of 107 conserved marker genes within open reading frames using mmgenome (Karst *et al.*, 2016), running BLASTP on the extracted marker genes against the RefSeq v.52 protein database with a maximum *e*-value cutoff of 1e-5, and finding the least common ancestor (LCA) of the top 5 blast hits for each marker gene with MEGAN v.6.4 (Huson *et al.*, 2007). The finest taxonomic ranking was assigned for which at least 70% of the LCA results agreed. Phylogenetic trees were generated for GBs that were over 40% complete using PhyloPhlAn v.1.3 based on 400 conserved marker genes (Segata *et al.*, 2013), as well as with UPGMA clustering of distance estimates from *in silico* DNA–DNA hybridization with the

Genome-to-Genome Distance Calculator v.2.1 (Auch *et al.*, 2010).

Statistical analysis

Statistically significant differences in raw read counts of OTUs (from 16S rRNA gene amplicon libraries) and GBs (from shotgun metagenome libraries) within the ^{12}C and ^{13}C DNA-SIP samples were detected with the negative binomial Wald test in DESeq2 v.1.14.1 separately for each codigester data set (Love *et al.*, 2014). Raw sequence counts of GBs were obtained from parsing the mapping files. An adjusted *P*-value of 0.01 and a $\log_2$ abundance increase greater than 2.0 (or >4-fold increase) were used to identify features (for example, OTUs or GBs) that significantly increased between the ^{12}C and ^{13}C DNA-SIP samples.

Regularized log-transformed sequence counts of 16S rRNA gene amplicon OTUs were determined with DESeq2 for use in principal component analysis. Permutational multivariate ANOVA (ADONIS) was conducted on Euclidian distance values from transformed sequence counts using the vegan package v.2.4.2 in R (Oksanen *et al.*, 2007).

Results

Conversion of oleate into methane and enrichment of ^{13}C DNA

Metabolism of ^{12}C- and ^{13}C-labeled oleate was confirmed with 97% and 95% COD recoveries as methane in the headspace for the PF codigester and CF codigester microcosms, respectively (Figure 1). Biokinetic modeling of methane production (described in Supplementary Information) showed that the maximum methane production rate increased with each subsequent batch feeding of ^{12}C- and ^{13}C-labeled oleate (Supplementary Table 1). The maximum methane production rate in the PF codigester microcosms was 26%, 21% and 17% higher than the CF codigester microcosms for the first, second and third batch incubation rounds, respectively (Supplementary Table 1).

Total DNA concentrations were measured in 24 density-gradient fractions to detect BD shifts after the consumption of 240 μmol ^{12}C- or ^{13}C-labeled oleate after 6 days. The heavy density fractions with BDs from 1.70 to 1.725 g ml^{-1} contained 2.2-times and 1.6-times more DNA in the ^{13}C-incubated samples than in the ^{12}C-controls for the PF and CF codigester microcosms, respectively (Supplementary Figure 2). To further confirm the enrichment of ^{13}C-labeled DNA, 16S rRNA genes of the LCFA-degrading bacterial genus *Syntrophomonas* were quantified in density fractions between 1.66 and 1.76 g ml^{-1} (Figure 2). The four heavy density-gradient fractions with BDs ranging from 1.70 to 1.725 g ml^{-1} contained over 12-times more *Syntrophomonas* 16S rRNA genes in the ^{13}C-incubated samples than that in the ^{12}C-controls for both codigesters (Figure 2). The four heavy gradient fractions showing high levels of ^{13}C incorporation were therefore pooled for each microcosm for subsequent 16S rRNA gene amplicon sequencing and shotgun metagenomic sequencing (Figure 2).

16S rRNA gene amplicon sequencing of DNA-SIP samples

The microbial community profiles of pooled heavy density-gradient fractions (Figure 2) were assessed through paired-end 16S rRNA gene amplicon sequencing. After qualify-filtering, denoising, and merging paired-end amplicon reads, the number of sequences retained per sample averaged 164 000 ± 39 000. Principal component analysis (PCA) showed that community profiles of heavy density fractions from the ^{12}C- and ^{13}C-incubated microcosms were distinctly clustered for both codigesters (Supplementary Figure 3). The grouping of community profiles was significant within both codigester sample sets according to the oleate isotope (ADONIS, $P<0.05$). Additionally, samples within each isotope group were significantly grouped according to the codigester sludge source (ADONIS, $P<0.05$), indicating that the ^{13}C-enriched communities from each codigester biomass were distinct.

Differential abundance analysis was conducted to detect 16S rRNA gene OTUs that significantly increased in ^{13}C-incubated heavy gradient fractions relative to ^{12}C-controls. A total of 59 differentially abundant OTUs were identified in the PF codigester samples, 42 of which were classified to the *Syntrophomonas* genus (Supplementary Figure 4). Within the CF codigester samples, a total of 40 differentially abundant OTUs were identified, with 36 classified as *Syntrophomonas* (Supplementary Figure 5). Of the total number of differentially abundant *Syntrophomonas* OTUs identified, 19 were shared between the codigesters while the remaining OTUs were unique to either codigester (Supplementary Figure 6). About 48 and 35% of the total 16S rRNA gene counts of differentially abundant *Syntrophomonas* OTUs were attributed to unique OTUs within the ^{13}C-samples for the CF and PF codigesters, respectively (Supplementary Figure 7). The relative fraction of *Syntrophomonas* 16S rRNA gene counts increased on average 2.6- and 2.9-times in the ^{13}C-incubated libraries relative to the ^{12}C-controls for the PF codigester and CF codigester, respectively (Figure 3). Cumulative *Syntrophomonas* genus 16S rRNA gene counts increased on average 5.0- and 5.5-times in the ^{13}C-incubated samples relative to the ^{12}C-controls for the PF codigester and CF codigester, respectively (Supplementary Figure 8). In contrast, the relative abundance of all other bacterial genera decreased in the ^{13}C 16S rRNA gene libraries relative to ^{12}C-controls for both codigesters, with the exception of the Ruminococcaceae NK4A214 group in the PF codigester (Figure 3). Other differentially

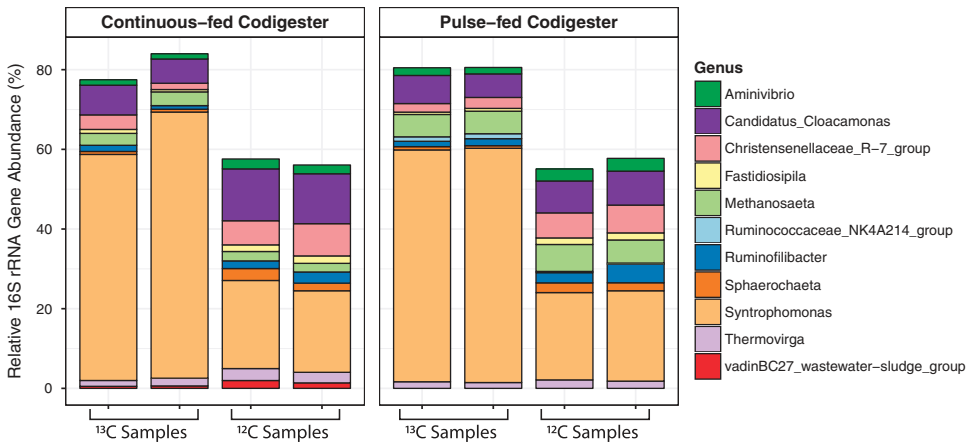

Figure 3 Relative fractions of the 11 most abundant genera in the heavy gradient fractions of ^{13}C-incubated samples and ^{12}C-controls for sample sets from both codigesters, based on 16S rRNA gene amplicon sequencing. Relative fractions were determined using DESeq2 normalized read counts for all OTUs (Love *et al*., 2014), and were then aggregated at the genus level. Both biological replicate microcosms are shown.

abundant OTUs were detected belonging to the genera: *Thermovirga, Aminivibrio,* Candidatus *Cloacamonas*, *Anaerofustis, Syntrophothermus* and *Ruminococcaceae* NK4A214 group, along with unclassified members of *Planctomycetes*, *Spirochaetae*, *Synergistes*, *Actinobacteria* and *Bacteriodetes* (Supplementary Figures 4 and 5). No methanogenic archaeal OTUs were identified as differentially abundant in either codigester sample set. Nonetheless, the relative abundance of *Methanosaeta* 16S rRNA genes increased from 2.2% in the ^{12}C-controls to 3.2% in the ^{13}C-samples for the CF codigester libraries (Figure 3). Cumulative 16S rRNA gene counts of *Methanosaeta* increased by 1.7- and 2.7-times in the ^{13}C-incubated samples relative to ^{12}C-controls for the PF codigester and CF codigester libraries, respectively, and *Methanobacterium* read counts increased by 1.7- and 1.9-times, respectively (Supplementary Figure 8).

DNA-SIP metagenomic sequencing

Metagenomes from the PF and CF codigester sludges before SIP incubation (that is, time zero) were assembled to produce contigs for differential coverage binning. The PF and CF codigester time zero metagenome assemblies amounted to 536 947 079 bp and 680 484 169 bp within contigs longer than 1 kb, and had maximum contig lengths of 692 259 bp and 485 835 bp, respectively. Over 200 GBs were recovered through differential coverage binning for each codigester DNA-SIP sample set. Differential abundance analysis of GB read counts in the ^{13}C-incubated metagenomes relative to ^{12}C-controls using DESeq2 showed that 16 and 18 GBs were significantly enriched in the ^{13}C-metagenomes of the PF and CF codigesters, respectively (Supplementary Table 2). Due to the low completeness of some enriched GBs (Supplementary Table 2), a threshold of 40% genome completeness was established for further phylogenetic analysis. Assigned taxonomies and genomic characteristics of differentially abundant GBs with over 40% completeness are summarized in Table 1.

Approximately 75% of the differentially abundant GBs (6 of 8) in the PF codigester samples were taxonomically assigned to *Syntrophomonas*, along with 71% (5 of 7) of the differentially abundant GBs in the CF codigester (Table 1). Both codigesters contained one differentially abundant GB that could only be assigned at the phylum-level to *Firmicutes*. In addition, one differentially abundant GB in the PF codigester was classified to the family-level of *Syntrophomonadaceae*, and one GB in the CF codigester was assigned to the phylum Candidatus *Parcubacteria* (Table 1). Multi-gene alignments based on a set of 400 conserved marker genes showed that some differentially abundant GBs from both codigesters were closely related, while each codigester also contained a set of unique ^{13}C-enriched GBs (Figure 4). GBs that formed sister groups based on both the conserved marker gene alignments and UPGMA clustering of *in silico* DNA–DNA hybridization distance values included *Syntrophomonas* sp. PF07 and *Syntrophomonas* sp. CF14, as well as *Syntrophomonas* sp. PF15 and *Syntrophomonas* sp. CF22 (Figure 4; Supplementary Figure 9). *Syntrophomonas* sp. PF103 was consistently clustered with the reference genomes of *Syntrophomonas wolfei* subsp. *wofei* and *Syntrophomonas wolfei* subsp. *methylbutyrica* (Figure 4; Supplementary Figure 9). *Firmicutes* sp. CF263 was placed on a branch outside of *Syntrophomonadaceae*-affiliated genomes based on marker gene alignments (Figure 4), yet it clustered with the reference genome of *Syntrophomonas zehnderi* OL-4 based on *in silico* DNA–DNA hybridization (Supplementary Figure 9). Both GBs of *Firmicutes* sp. PF36 and Candidatus *Parcubacteria* sp. CF250 were placed as outgroups in both phylogenetic clustering approaches (Figure 4, Supplementary Figure S9).

Table 1 Taxonomic classification and characteristics for genome bins that were significantly enriched ($P<0.01$, $\log_2$ increase >2.0) in ^{13}C-metagenomes relative to ^{12}C-controls for both codigester sample sets

Genome bin I.D.	*Taxonomy*[a]	*Assigned bin 'Species' name*	*Completeness*[b]	*GC*	*Size (Mbp)*	*Coding density*[b]
Pulse-fed Codigester Genome Bins						
bin.15	*Syntrophomonas*	*Syntrophomonas* sp. PF15	47%	41.4%	1.21	86%
bin.75	*Syntrophomonas*	*Syntrophomonas* sp. PF75	90%	41.2%	2.10	89%
bin.62	*Syntrophomonas*	*Syntrophomonas* sp. PF62	97%	43.5%	2.66	87%
bin.103	*Syntrophomonas*	*Syntrophomonas* sp. PF103	57%	44.6%	1.12	85%
bin.36	*Firmicutes*	*Firmicutes* sp. PF36	85%	50.8%	1.60	90%
bin.111	*Syntrophomonas*	*Syntrophomonas* sp. PF111	89%	45.7%	3.38	88%
bin.7	*Syntrophomonas*	*Syntrophomonas* sp. PF07	74%	49.7%	1.27	89%
bin.128	*Syntrophomonadaceae*	*Syntrophomonadaceae* sp. PF128	98%	46.4%	2.71	88%
Continuous-fed Codigester Genome Bins						
bin.22	*Syntrophomonas*	*Syntrophomonas* sp. CF22	74%	41.4%	2.00	86%
bin.196	*Syntrophomonas*	*Syntrophomonas* sp. CF196	72%	42.9%	2.41	87%
bin.226	*Syntrophomonas*	*Syntrophomonas* sp. CF226	98%	47.6%	3.18	88%
bin.14	*Syntrophomonas*	*Syntrophomonas* sp. CF14	63%	49.7%	0.78	89%
bin.263	*Firmicutes*	*Firmicutes* sp. CF263	83%	50.6%	4.81	92%
bin.250	Candidatus *Parcubacteria*	Candidatus *Parcubacteria* sp. CF250	40%	30.8%	0.25	91%
bin.187	*Syntrophomonas*	*Syntrophomonas* sp. CF187	86%	45.6%	2.12	89%

Only genome bins that were above 40% completion are included.
[a]Based on LCA of BLAST output.
[b]Based on CheckM output.

The largest GB coverage fold-change in the ^{13}C-incubated samples was observed for the sister group of *Syntrophomonas* sp. PF15 & *Syntrophomonas* sp. CF22, which were not closely related to previously-sequenced *Syntrophomonas* isolates (Figure 4; Supplementary Table 2). Other GBs that had high fold-changes in the ^{13}C-incubated samples ($\log_2$ change >3.0) included *Syntrophomonas* sp. PF75, *Syntrophomonas* sp. PF62, *Syntrophomonas* sp. PF103, *Firmicutes* sp. PF36, *Syntrophomonas* sp. PF111, and *Syntrophomonas* sp. CF196 (Figure 4; Supplementary Table 2). In comparison to the CF codigester, the PF codigester had a greater number of GBs that were enriched above a $\log_2$ change of 3.0 in the ^{13}C-incubated samples (Figure 4).

To assess the functional potential of differentially abundant GBs in ^{13}C-incubated samples, coverage values were extracted and summarized for KEGG ECs within the LCFA degradation pathway (KEGG Pathway Map 00071). Long-chain fatty acid CoA ligase (EC:6.2.1.3), which is responsible for activating free-fatty acids to acyl-CoA thioesters (Sousa *et al*., 2009), had the highest EC coverage in differentially abundant GBs within ^{13}C-samples from both codigesters (Figure 5). The EC categories with the next highest coverage were enoyl-CoA hydratase (EC:4.2.1.17) and acetyl-CoA acetyltransferase (EC:2.3.1.9). Genes encoding for the entire fatty acid β-oxidation cycle were identified within the differentially abundant GBs for both codigesters (Figure 5). However, genes for acyl-CoA dehydrogenase (EC: 1.3.99.-) were observed in the PF codigester GBs but not in the CF codigester GBs (Figure 5). The GBs in the PF codigester also had substantially higher gene coverage for 3-hydroxyacyl-CoA dehydrogenases (EC:1.1.1.35 and EC:1.1.1.36) in ^{13}C-incubated samples than the CF codigester GBs (Figure 5). Additionally, genes encoding for Δ^2,Δ^4-dienoyl-CoA reductase (EC:1.3.1.34) involved in the metabolism of unsaturated fatty acids (Ren *et al*., 2004) were detected in the differentially abundant GBs for both codigesters, and had a coverage that was an order of magnitude higher in the PF codigester GBs (Supplementary Table 3).

Syntrophic conversion of LCFA under methanogenic conditions involves interspecies electron transfer between *Bacteria* and *Archaea*, which commonly involves hydrogen and/or formate as electron shuttles (Stams and Plugge, 2009). Several formate dehydrogenases and hydrogenases were detected in the enriched GBs of both codigesters (Supplementary Figure 10). Formate dehydrogenases (EC:1.2.1.2, EC:1.2.1.43) were more abundant than hydrogenases (EC:1.12.1.2, EC:1.12.7.2, EC:1.12.1.3), and had similar coverage in the differentially abundant GBs from both codigesters (Supplementary Figure 10). In contrast, hydrogenases (EC:1.12.1.2, EC:1.12.1.3) had lower coverage in the CF codigester GBs relative to the PF codigester (Supplementary Figure 10).

Discussion

This research conducted a genome-centric comparison of the active populations between two anaerobic codigesters that were either pulse-fed or continuously-fed with oleate. DNA-SIP was combined with shotgun metagenomic sequencing and differential coverage binning to provide novel insights into active LCFA-degrading populations, and highlighted the potential for physiological

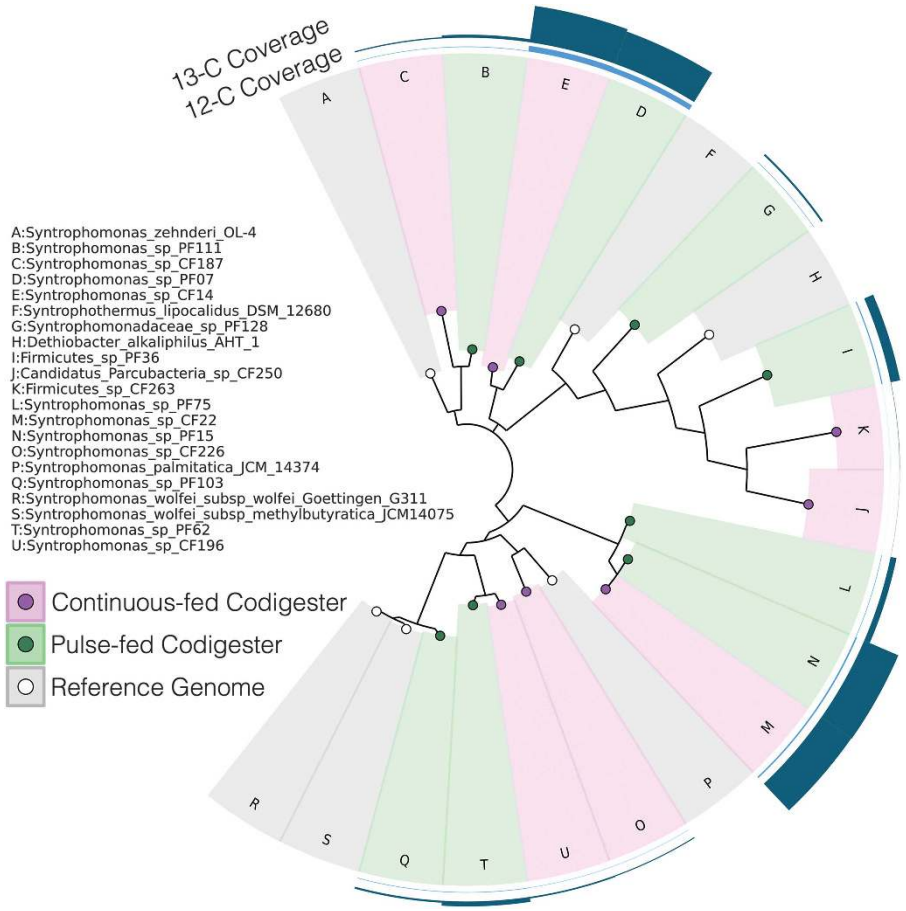

Figure 4 Phylogenetic overview of differentially abundant genome bins identified in both anaerobic codigester DNA-SIP metagenomes. The tree was constructed based on a concatenated alignment of conserved marker genes within the metagenomic contigs of each bin using PhyloPhlAn v.1.3 (Segata *et al.*, 2013). The color of each genome bin node represents the codigester biomass source, and the height of the outer bars represent the genome bin coverage in the heavy gradient fractions of the ^{13}C-incubated samples and ^{12}C-controls. The tree was illustrated using GraPhLan v.0.9.7 (Asnicar *et al.*, 2015).

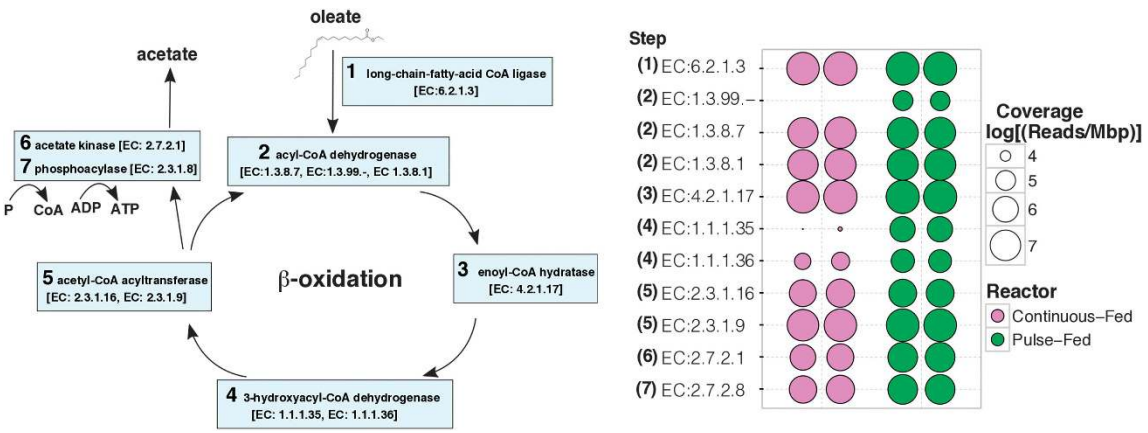

Figure 5 Cumulative coverage values of KEGG ECs potentially involved in LCFA degradation (KEGG map 00071), based on the coverage of all differentially abundant genome bins in the ^{13}C-incubated DNA-SIP metagenomes. Values from duplicate biological replicates are shown for both codigesters, and the size of each marker is proportional to the $\log_{10}$ of the EC read coverage.

diversity at the trophic level of syntrophy within anaerobic digesters.

As the average specific growth rate (μ) in the codigesters was 0.05 d^{-1} based on the 20-d SRT, higher growth rates would have been needed for cell duplication and sufficient DNA labeling during the 6-d incubation time, which could have been promoted by batch feeding oleate at initial concentrations of 8 mM in the SIP incubations. A growth rate of 0.11 d^{-1} would be required for cell doubling within a

6-d period, which is within the range of maximum specific growth rates (μ_{max}) for co-cultures of syntrophic fatty acid oxidizing bacteria and methanogenic archaea of 0.10 to 0.19 d^{-1} (Stams *et al.*, 2012). While a longer incubation time would have contributed to further DNA labeling, longer incubation times in DNA-SIP can be problematic because they can lead to cross-labeling of peripheral populations due to endogenous cell decay (Neufeld *et al.*, 2006). In contrast to our study, previous studies employing DNA-SIP for syntrophic propionate- and butyrate-degrading communities in soil utilized incubation times ranging from 17 to 69 days (Lueders *et al.*, 2004; Chauhan and Ogram, 2006; Liu *et al.*, 2011; Gan *et al.*, 2012; Li *et al.*, 2015b). These longer incubation times may have been necessitated due to the low active biomass fractions in soil, which would result in low substrate conversion rates. The higher active syntrophic biomass fraction in the anaerobic codigester sludges in this study promoted more rapid oleate bioconversion in the microcosms, which permitted efficient DNA-SIP labeling within a 6- day incubation period. DNA-SIP based metagenomics could thus be potentially applied with relatively short SIP incubation times to study other biological wastewater treatment process that have relatively high active biomass fractions.

Syntrophic fatty acid conversion requires that free energy from catabolism is shared between syntrophic bacteria and methanogenic archaeal partners (Schink, 1997; Stams and Plugge, 2009). In this study, all of the 16S rRNA gene OTUs that were differentially abundant in ^{13}C-incubated DNA-SIP samples for both codigesters belonged to the domain *Bacteria*, while no *Archaea* OTUs were differentially abundant in ^{13}C-incubated samples. Likewise, all of the differentially abundant GBs recovered from the DNA-SIP shotgun metagenomes were assigned to bacterial taxa. However, the higher cumulative 16S rRNA gene read counts of *Methanosaeta* and *Methanobacterium* in ^{13}C-incubated samples relative to ^{12}C-controls indicates that they were likely methanogenic partners involved in syntrophic oleate degradation in both codigesters, but the increases in their OTU abundances were not statistically significant. The relatively high level of ^{12}C-background substrates for methanogenesis (from the digester inoculum) likely diluted the ^{13}C-labeled DNA of methanogenic archaea, as was also observed with protein-SIP in anaerobic digester communities (Mosbæk *et al.*, 2016).

To the best of our knowledge, this is the first study to couple DNA-SIP with differential coverage binning to recover population GBs from environmental metagenomes. Differential abundance analysis of GB read counts was an effective technique coupled to DNA-SIP metagenomic binning to identify GBs that were significantly enriched within the heavy gradient fractions of ^{13}C-incubated samples versus ^{12}C-controls. The taxonomic assignment of differentially abundant GBs agreed with the results of 16S rRNA gene amplicon sequencing, as over 70% of the GBs belonged to the genus *Syntrophomonas*. This finding corroborates previous indications that *Syntrophomonas* are key syntrophic LCFA-degrading bacteria in mesophilic anaerobic digesters (Shigematsu *et al.*, 2006; Hatamoto *et al.*, 2007; Sousa *et al.*, 2007, 2009; Ziels *et al.*, 2015). However, this is the first study to determine the relative contribution of *Syntrophomonas* toward LCFA degradation using DNA-SIP. The finding that some phylogenetically distinct *Syntrophomonas* GBs and 16S rRNA gene OTUs were unique to each codigester further suggests that microbial communities involved in LCFA conversion can be physiologically diverse, and that the LCFA feeding frequency selected for unique active LCFA-degrading syntrophic taxa. Syntrophic bacteria have traditionally been considered metabolic-specialists (McInerney *et al.*, 2009; Sieber *et al.*, 2012), which has led to the general conclusion that they have low functional redundancy in anaerobic digesters (Werner *et al.*, 2011; Carballa *et al.*, 2015). A previous genome-centric analysis of anaerobic digester metagenomes found low diversity within the trophic level of syntrophic acetogenesis (Vanwonterghem *et al.*, 2016). Using transcriptomic read mapping, Treu *et al.* (2016a) could only identify two active *Syntrophomonas* GBs in an anaerobic digester after pulsing oleate. In this study, 12 active *Syntrophomonas* GBs were identified using targeted DNA-SIP metagenomic analysis. DNA-SIP based metagenomic binning may thus improve our resolution of anaerobic digester trophic groups by enriching metagenome libraries with actively growing population genomes (Coyotzi *et al.*, 2016), which may be especially useful to study low-abundance groups like syntrophic bacteria (Stams *et al.*, 2012). The recent recovery of 236 microbial GBs from anaerobic digester metagenomes led to conclusion that *Syntrophomonas* were among a core essential microbial group that is present independent of digester operational conditions (Treu *et al.*, 2016b). Our finding that the anaerobic digester feeding frequency can impact the genomic composition of *Syntrophomonas* thus has implications for developing operating strategies that steer the core digester community to obtain better biokinetics and process stability.

In prior research, it was observed that the frequency of LCFA feeding led to different biokinetics between the PF and CF codigesters, which were correlated with individual *Syntrophomonas* taxa abundances between the two systems (Ziels *et al.*, 2017). In this study, biokinetic modeling of methane production in the DNA-SIP microcosms fed with either ^{13}C- or ^{12}C- oleate showed that the PF codigester sludge had higher maximum oleate conversion rates than CF codigester sludge during all three DNA-SIP batch degradation periods. This result further corroborates that biological selection from the LCFA feeding frequency altered LCFA bioconversion kinetics in the anaerobic codigesters

(Ziels *et al*., 2017). The different oleate bioconversion kinetics observed between the two codigesters could have been attributed to differences in the functional gene repertoires of their active LCFA-degrading populations. The differentially abundant GBs in the PF codigester had more redundant KEGG ECs (for example, multiple ECs for a single reaction step) in the LCFA degradation pathway compared to the CF codigester GBs, which could indicate that pulse feeding led to a higher level of metabolic flexibility. The PF codigester GBs also had a greater distribution of formate dehydrogenase and hydrogenase encoding genes, which have been suggested to afford syntrophs with metabolic flexibility in fluctuating environmental conditions (Meyer *et al*., 2013; Sieber *et al*., 2014). The greater metabolic flexibility identified in the ^{13}C-enriched GBs of the PF codigester in this study suggests that pulse feeding could promote a greater physiological adaptive capacity by supporting a higher level of functional redundancy within the ecological niches of anaerobic digesters, which in turn may have supported its higher oleate loading tolerance (Ziels *et al*., 2017). A greater tolerance to overloading and toxicity has also been observed in other pulse-fed anaerobic digesters compared to continuous-fed systems (Conklin *et al*., 2006; De Vrieze *et al*., 2013; Mulat *et al*., 2016). Although stochastic processes cannot be ruled out because the bioreactors were not replicated, the fact that these bioreactors were inoculated with the same seed source and *Syntrophomonas* was the predominant group impacted by oleate addition for over 230 days (Ziels *et al*., 2017) indicates that the feeding frequency likely imparted a deterministic selective pressure on the syntrophic community structure.

In summary, this study demonstrated the application of DNA-SIP combined with metagenomics and differential coverage binning to identify active populations in an engineered biological treatment process. The results indicated that the operating conditions, specifically the feeding frequency, of the methanogenic bioreactors impacted the genomic composition of active syntrophic populations. The feeding frequency also impacted the level of functional gene redundancy within the active populations, which had implications for increased physiological adaptation using a pulse feeding strategy. Thus, DNA-SIP metagenomics is a powerful tool to help understand how operating strategies may improve the performance of biological wastewater treatment processes, as was shown here for increased methane recovery from high-strength organic wastes.

Conflict of Interest

The authors declare no conflict of interest.

Acknowledgements

We thank David Stahl for his helpful input and review of this manuscript. This research was funded by the US EPA STAR [grant RD835567] (RMZ and HDS), the US DOE JGI [grant CSP 2791] (DACB), and the ERC [grant 323009] (DZS).

References

Albertsen M, Hugenholtz P, Skarshewski A, Nielsen KL, Tyson GW, Nielsen PH. (2013). Genome sequences of rare, uncultured bacteria obtained by differential coverage binning of multiple metagenomes. *Nat Biotechnol* **31**: 533–538.

Alves MM, Pereira MA, Sousa DZ, Cavaleiro AJ, Picavet M, Smidt H *et al*. (2009). Waste lipids to energy: how to optimize methane production from long-chain fatty acids (LCFA). *Microb Biotechnol* **2**: 538–550.

Angelidaki I, Ahring BK. (1992). Effects of free long-chain fatty acids on thermophilic anaerobic digestion. *Appl Microbiol Biotechnol* **37**: 808–812.

Asnicar F, Weingart G, Tickle TL, Huttenhower C, Segata N. (2015). Compact graphical representation of phylogenetic data and metadata with GraPhlAn. *Peer J* **3**: e1029.

Auch AF, von Jan M, Klenk H-P, Göker M. (2010). Digital DNA-DNA hybridization for microbial species delineation by means of genome-to-genome sequence comparison. *Stand Genomic Sci* **2**: 117–134.

Briones A, Raskin L. (2003). Diversity and dynamics of microbial communities in engineered environments and their implications for process stability. *Curr Opin Biotechnol* **14**: 270–276.

Callahan BJ, McMurdie PJ, Rosen MJ, Han AW, Johnson AJA, Holmes SP. (2016). DADA2: High-resolution sample inference from Illumina amplicon data. *Nat Methods* **13**: 581–583.

Carballa M, Regueiro L, Lema JM. (2015). Microbial management of anaerobic digestion: exploiting the microbiome-functionality nexus. *Curr Opin Biotechnol* **33**: 103–111.

Chauhan A, Ogram A. (2006). Fatty acid-oxidizing consortia along a nutrient gradient in the Florida Everglades. *Appl Environ Microbiol* **72**: 2400–2406.

Chemerys A, Pelletier E, Cruaud C, Martin F, Violet F, Jouanneau Y. (2014). Characterization of novel polycyclic aromatic hydrocarbon dioxygenases from the bacterial metagenomic DNA of a contaminated soil. *Appl Environ Microbiol* **80**: 6591–6600.

Chen I-MA, Markowitz VM, Chu K, Palaniappan K, Szeto E, Pillay M *et al.* (2016). IMG/M: integrated genome and metagenome comparative data analysis system. *Nucleic Acids Res* **45**: D507–D516.

Chen Y, Murrell JC. (2010). When metagenomics meets stable-isotope probing: progress and perspectives. *Trends Microbiol* **18**: 157–163.

Conklin A, Stensel HD, Ferguson J. (2006). Growth kinetics and competition between methanosarcina and methanosaeta in mesophilic anaerobic digestion. *Water Environ Res* **78**: 486–496.

Coyotzi S, Pratscher J, Murrell JC, Neufeld JD. (2016). Targeted metagenomics of active microbial populations with stable-isotope probing. *Curr Opin Biotechnol* **41**: 1–8.

Davidsson Å, Lövstedt C, la Cour Jansen J, Gruvberger C, Aspegren H. (2008). Co-digestion of grease trap sludge and sewage sludge. *Waste Manag* **28**: 986–992.

De Vrieze J, Verstraete W, Boon N. (2013). Repeated pulse feeding induces functional stability in anaerobic digestion. *Microb Biotechnol* **6**: 414–424.

Dumont MG, Murrell JC. (2005). Stable isotope probing — linking microbial identity to function. *Nat Rev Microbiol* **3**: 499–504.

Edgar RC. (2013). UPARSE: highly accurate OTU sequences from microbial amplicon reads. *Nat Methods* **10**: 996–998.

Eyice Ö, Namura M, Chen Y, Mead A, Samavedam S, Schäfer H. (2015). SIP metagenomics identifies uncultivated Methylophilaceae as dimethylsulphide degrading bacteria in soil and lake sediment. *ISME J* **9**: 2336–2348.

Gan Y, Qiu Q, Liu P, Rui J, Lu Y. (2012). Syntrophic oxidation of propionate in rice field soil at 15 and 30 °C under methanogenic conditions. *Appl Environ Microbiol* **78**: 4923–4932.

Guo M, Song W, Buhain J. (2015). Bioenergy and biofuels: History, status, and perspective. *Renew Sustain Energy Rev* **42**: 712–725.

Hanaki K, Matsuo T, Nagase M. (1981). Mechanism of inhibition caused by long-chain fatty acids in anaerobic digestion process. *Biotechnol Bioeng* **23**: 1591–1610.

Hatamoto M, Imachi H, Ohashi A, Harada H. (2007). Identification and cultivation of anaerobic, syntrophic long-chain fatty acid-degrading microbes from mesophilic and thermophilic methanogenic sludges. *Appl Environ Microbiol* **73**: 1332–1340.

Huson DH, Auch AF, Qi J, Schuster SC. (2007). MEGAN analysis of metagenomic data. *Genome Res* **17**: 377–386.

Kang DD, Froula J, Egan R, Wang Z. (2015). MetaBAT, an efficient tool for accurately reconstructing single genomes from complex microbial communities. *PeerJ* **3**: e1165.

Karst SM, Kirkegaard RH, Albertsen M. (2016). mmgenome: a toolbox for reproducible genome extraction from metagenomes. *BioRxiv*, doi:https://doi.org/10.1101/059121.

Li D, Liu C-M, Luo R, Sadakane K, Lam T-W. (2015a). MEGAHIT: an ultra-fast single-node solution for large and complex metagenomics assembly via succinct de Bruijn graph. *Bioinformatics* **31**: 1674–1676.

Li H, Chang J, Liu P, Fu L, Ding D, Lu Y. (2015b). Direct interspecies electron transfer accelerates syntrophic oxidation of butyrate in paddy soil enrichments. *Environ Microbiol* **17**: 1533–1547.

Li H, Handsaker B, Wysoker A, Fennell T, Ruan J, Homer N *et al.* (2009). The Sequence Alignment/Map format and SAMtools. *Bioinformatics* **25**: 2078–2079.

Liu P, Qiu Q, Lu Y. (2011). Syntrophomonadaceae-affiliated species as active butyrate-utilizing syntrophs in paddy field soil. *Appl Environ Microbiol* **77**: 3884–3887.

Love MI, Huber W, Anders S. (2014). Moderated estimation of fold change and dispersion for RNA-seq data with DESeq2. *Genome Biol* **15**: 1.

Lueders T, Pommerenke B, Friedrich MW. (2004). Stable-isotope probing of microorganisms thriving at thermodynamic limits: syntrophic propionate oxidation in flooded soil. *Appl Environ Microbiol* **70**: 5778–5786.

Luostarinen S, Luste S, Sillanpää M. (2009). Increased biogas production at wastewater treatment plants through co-digestion of sewage sludge with grease trap sludge from a meat processing plant. *Bioresour Technol* **100**: 79–85.

McInerney MJ, Sieber JR, Gunsalus RP. (2009). Syntrophy in anaerobic global carbon cycles. *Curr Opin Biotechnol* **20**: 623–632.

Meyer B, Kuehl JV, Deutschbauer AM, Arkin AP, Stahl DA. (2013). Flexibility of syntrophic enzyme systems in desulfovibrio species ensures their adaptation capability to environmental changes. *J Bacteriol* **195**: 4900–4914.

Mosbæk F, Kjeldal H, Mulat DG, Albertsen M, Ward AJ, Feilberg A *et al.* (2016). Identification of syntrophic acetate-oxidizing bacteria in anaerobic digesters by combined protein-based stable isotope probing and metagenomics. *ISME J* **10**: 2405–2418.

Mulat DG, Jacobi HF, Feilberg A, Adamsen APS, Richnow H-H, Nikolausz M. (2016). Changing feeding regimes to demonstrate flexible biogas production: effects on process performance, microbial community structure, and methanogenesis pathways. *Appl Environ Microbiol* **82**: 438–449.

Neufeld JD, Dumont MG, Vohra J, Murrell JC. (2006). Methodological considerations for the use of stable isotope probing in. *Microb Ecol* **53**: 435–442.

Oksanen J, Kindt R, Legendre P, O'Hara B, Stevens MHH, Oksanen MJ *et al.* (2007). The vegan package. *Community Ecol Package* **10**: 631–637.

Parada AE, Needham DM, Fuhrman JA. (2016). Every base matters: assessing small subunit rRNA primers for marine microbiomes with mock communities, time series and global field samples. *Environ Microbiol* **18**: 1403–1414.

Parks DH, Imelfort M, Skennerton CT, Hugenholtz P, Tyson GW. (2015). CheckM: assessing the quality of microbial genomes recovered from isolates, single cells, and metagenomes. *Genome Res* **25**: 1043–1055.

Radajewski S, Ineson P, Parekh NR, Murrell JC. (2000). Stable-isotope probing as a tool in microbial ecology. *Nature* **403**: 646–649.

Ren Y, Aguirre J, Ntamack AG, Chu C, Schulz H. (2004). An alternative pathway of oleate β-oxidation in *Escherichia coli* involving the hydrolysis of a dead end intermediate by a thioesterase. *J Biol Chem* **279**: 11042–11050.

Rinzema A, Boone M, Knippenberg K, van, Lettinga G. (1994). Bactericidal effect of long chain fatty acids in anaerobic digestion. *Water Environ Res* **66**: 40–49.

Saidi-Mehrabad A, He Z, Tamas I, Sharp CE, Brady AL, Rochman FF *et al.* (2013). Methanotrophic bacteria in oilsands tailings ponds of northern Alberta. *ISME J* **7**: 908–921.

Schink B. (1997). Energetics of syntrophic cooperation in methanogenic degradation. *Microbiol Mol Biol Rev* **61**: 262–280.

Segata N, Börnigen D, Morgan XC, Huttenhower C. (2013). PhyloPhlAn is a new method for improved phylogenetic and taxonomic placement of microbes. *Nat Commun* **4**: 2304.

Shigematsu T, Tang Y, Mizuno Y, Kawaguchi H, Morimura S, Kida K. (2006). Microbial diversity of mesophilic methanogenic consortium that can degrade long-chain fatty acids in chemostat cultivation. *J Biosci Bioeng* **102**: 535–544.

Sieber JR, Le HM, McInerney MJ. (2014). The importance of hydrogen and formate transfer for syntrophic fatty, aromatic and alicyclic metabolism. *Environ Microbiol* **16**: 177–188.

Sieber JR, McInerney MJ, Gunsalus RP. (2012). Genomic insights into syntrophy: the paradigm for anaerobic metabolic cooperation. *Annu Rev Microbiol* **66**: 429–452.

Sousa DZ, Pereira MA, Smidt H, Stams AJM, Alves MM. (2007). Molecular assessment of complex microbial communities degrading long chain fatty acids in methanogenic bioreactors. *FEMS Microbiol Ecol* **60**: 252–265.

Sousa DZ, Smidt H, Alves MM, Stams AJM. (2009). Ecophysiology of syntrophic communities that degrade saturated and unsaturated long-chain fatty acids. *FEMS Microbiol Ecol* **68**: 257–272.

Stams AJM, Plugge CM. (2009). Electron transfer in syntrophic communities of anaerobic bacteria and archaea. *Nat Rev Microbiol* **7**: 568–577.

Stams AJM, Sousa DZ, Kleerebezem R, Plugge CM. (2012). Role of syntrophic microbial communities in high-rate methanogenic bioreactors. *Water Sci Technol* **66**: 352.

Sundberg C, Al-Soud WA, Larsson M, Alm E, Yekta SS, Svensson BH *et al.* (2013). 454 pyrosequencing analyses of bacterial and archaeal richness in 21 full-scale biogas digesters. *FEMS Microbiol Ecol* **85**: 612–626.

Treu L, Campanaro S, Kougias PG, Zhu X, Angelidaki I. (2016a). Untangling the effect of fatty acid addition at species level revealed different transcriptional responses of the biogas microbial community members. *Environ Sci Technol* **50**: 6079–6090.

Treu L, Kougias PG, Campanaro S, Bassani I, Angelidaki I. (2016b). Deeper insight into the structure of the anaerobic digestion microbial community; the biogas microbiome database is expanded with 157 new genomes. *Bioresour Technol* **216**: 260–266.

Vanwonterghem I, Jensen PD, Ho DP, Batstone DJ, Tyson GW. (2014). Linking microbial community structure, interactions and function in anaerobic digesters using new molecular techniques. *Curr Opin Biotechnol* **27**: 55–64.

Vanwonterghem I, Jensen PD, Rabaey K, Tyson GW. (2016). Genome-centric resolution of microbial diversity, metabolism and interactions in anaerobic digestion. *Environ Microbiol* **18**: 3144–3158.

Verastegui Y, Cheng J, Engel K, Kolczynski D, Mortimer S, Lavigne J *et al.* (2014). Multisubstrate isotope labeling and metagenomic analysis of active soil bacterial communities. *mBio* **5**: e01157–14.

Wan C, Zhou Q, Fu G, Li Y. (2011). Semi-continuous anaerobic co-digestion of thickened waste activated sludge and fat, oil and grease. *Waste Manag* **31**: 1752–1758.

Wang L, Aziz TN, de los Reyes FL. (2013). Determining the limits of anaerobic co-digestion of thickened waste activated sludge with grease interceptor waste. *Water Res* **47**: 3835–3844.

Werner JJ, Knights D, Garcia ML, Scalfone NB, Smith S, Yarasheski K *et al.* (2011). Bacterial community structures are unique and resilient in full-scale bioenergy systems. *Proc Natl Acad Sci USA* **108**: 4158–4163.

Zhang F, Liu X, Dong X. (2012). Thermosyntropha tengcongensis sp. nov., a thermophilic bacterium that degrades long-chain fatty acids syntrophically. *Int J Syst Evol Microbiol* **62**: 759–763.

Ziels RM, Beck DAC, Martí M, Gough HL, Stensel HD, Svensson BH. (2015). Monitoring the dynamics of syntrophic β-oxidizing bacteria during anaerobic degradation of oleic acid by quantitative PCR. *FEMS Microbiol Ecol* **91**: fiv028.

Ziels RM, Karlsson A, Beck DAC, Ejlertsson J, Yekta SS, Bjorn A *et al.* (2016). Microbial community adaptation influences long-chain fatty acid conversion during anaerobic codigestion of fats, oils, and grease with municipal sludge. *Water Res* **103**: 372–382.

Ziels RM, Beck DAC, Stensel HD. (2017). Long-chain fatty acid feeding frequency in anaerobic codigestion impacts syntrophic community structure and biokinetics. *Water Res* **111**: 218–229.

Supplementary Information accompanies this paper on The ISME Journal website (http://www.nature.com/ismej)